NONLINEAR METHOD OF PRECRASH VELOCITY DETERMINATION FOR MINI CAR CLASS-B-SPLINE TENSORS PRODUCTS WITH PROBABILISTIC WEIGHTS

ADAM MROWICKI[1], PRZEMYSŁAW KUBIAK[2], WOJCIECH ZAKRZEWICZ[3]

Abstract

Following paper introduces the nonlinear method of determining the velocity of a vehicle before the impact-the Equivalent Energy Speed (EES). To estimate the magnitude of EES, the method utilizes the deformation work Wdef of the vehicle, defined by the quotient of deformation coefficient C_s and plastic deformation. Combined with the introduction of the B-spline tensor products and least square approximation with probabilistic weights, method shows promising results.

Keywords: crash test; EES; precrash velocity; nonlinear; deformation work

1. Introduction

The three main factors deciding a road accident are: driver, vehicle and road conditions. Therefore, the most common causes of vehicle accidents are strictly related to those factors: driver's lack of attention, forcing the right of way, inadequate sight distance, noncompliance with traffic lights, inadequate speed when adverse driving conditions are present [2, 21, 22, 27]. When examining a road accident, an investigator has to collect data and analyze many variables, but one of the most crucial one is the vehicle velocity. Method of its determination is the main aspect of accident reconstruction.

Currently, the most popular methods of precrash velocity determination utilize a linear model [6, 7, 37]. This approach is based on an assumption that b_k coefficient is the slope of deformation coefficient C_s [20, 36] and vehicle mass m. Such simplification comes with a higher error of velocity estimation [18, 19]. Therefore an alternative method was devised-a nonlinear approach. This new method is based on three main assumptions:

[1] Institute of Machine Design and Operation, Wroclaw University of Technology, I. Łukasiewicza 7/9, 50-371 Wroclaw, Poland, e-mail: mrowicki.adam@gmail.com

[2] Institute of Vehicles, Warsaw University of Technology, Ludwika Narbutta 84, 02-524 Warszawa, Poland, e-mail: przemyslaw.kubiak@pw.edu.pl

[3] Institute of Vehicles, Warsaw University of Technology, Ludwika Narbutta 84, 02-524 Warszawa, Poland, e-mail: wojciech.zakrzewicz.dokt@pw.edu.pl

- b_k slope of nonlinearly dependent on C_s deformation and vehicle mass m.
- b_k slope is nonlinearly dependent on dent zone width L_t [9, 17, 24, 25].
- it is possible to divide all cases into categories dependent on vehicle size, as in Table 1.

Tab. 1. Mini vehicle class conditions

Class	Mini
Wheel base [mm]	≤2408
Wheel track [mm]	≤1298
Length [mm]	≤4059
Width [mm]	≤1544
Mass [kg]	≤900

The mathematical model for this new approach was developed based on NHTSA database C [28, 29]. National Highway and Traffic Safety Agency, among others, enforces the Federal Motor Vehicle Safety Standards and assesses the safety of vehicles in US. The assessment is based on numerous crash tests performed by NHTSA. Among those tests there are the frontal collision crash tests that are the scope of this method. As mentioned above, vehicles can be divided into categories and the NHTSA database allows for a division based on vehicles' weight.

The nonlinear model is based on deformation work of the collision. The EES value [5, 30, 31, 34] can be found using the following equation (1):

$$EES = \sqrt{\frac{2 \cdot W_{def}}{m}} \tag{1}$$

Finding the EES velocity begins with determining the amount of energy used on plastic deformation of the chassis [30, 31, 35]. For this purpose, the vehicle's deformation profile has to be defined. In case of frontal impact, the front part of chassis is designed to absorb most of the energy and convert it into deformation. To increase the accuracy, it is advised to perform measurements of the deformation in 6 points as shown in Figure 1.

Due to a nonuniform structure of vehicle chassis, a smaller number of points would lead to greater error of measurement [13, 14, 15].

Having the values for all points, the overall coefficient of deformation C_s [4, 8, 16, 23] can be determined, according to formula (2):

$$C_s = \frac{\frac{C_1}{2} + (C_2 + C_3 + C_4 + C_5) + \frac{C_6}{2}}{n-1} \tag{2}$$

n-number of deformation measurement points.

The deformation coefficient serves to calculate the constant stiffness b_k, according to formula (3):

$$b_k = \frac{v_t - b_{sg}}{C_s} \tag{3}$$

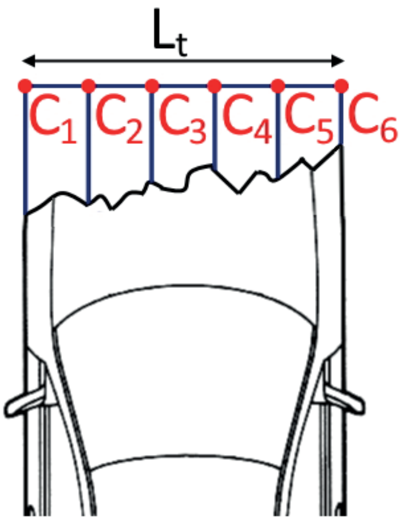

Fig. 1. Deformation measurement points $C_{1\text{-}6}$ and deformation zone L_t

2. Nonlinear approach

The dependencies presented in prior section govern the crash site reconstruction and lay the base for the nonlinear method. NHTSA tests that were taken into consideration when preparing the model were frontal collision at 50 km/h. The most crucial difference between the linear and nonlinear approach is the assumption of the EES speed and deformation C_S relationship [10, 12]. To simplify the calculations and thus increase the computation speed this dependency, up till now, was assumed to be linear. This does not have to be the case as, according to Moore's law, the number of transistors on integrated circuit chips doubles every two years. Such linear assumption decreases the level of overall accuracy, therefore Author developed a method that assumes nonlinear behavior of EES and C_S ratio dependence.

Author searches for simplifications in different areas that would not create any negative impact on the accuracy. One of such areas is the approach to compute the deformation work W_{def}. Instead of calculating subsequent coefficients, Author uses a known algebraic form to determine the value for W_{def}. Such formula was devised based on experimental data and nonlinear algorithms. From the viewpoint of computing, such estimation is much less resource intensive, yet as accurate as the traditional approach.

Moreover, Author together with Associates plans to develop a device that would estimate the precrash velocity instantly. Such device is going to use lasers to scan the deformed surface of the vehicle and determine the deformation ratio C_S. Alternatively, such device could take advantage of recently emerging technology of photogrammetry, where the investigator would only have to take photographs of deformed car body from different angles. Then the software would join several pictures into one three dimensional object and determine the dent zone and subsequent deformation coefficients.

The b_k coefficient is the slope of EES and C_s relation. When the relation is linear, it defines the initial value of EES, i.e. when the C_s deformation ratio coefficient is equal to 0 and only elastic deformation are present. For the purpose of calculations, the speed at which plastic deformation occur b_{sg} was assumed to be 3.05 m/s or 11 km/h.

Quite vital issue, often neglected, is non-centricity of deformation coefficients C_1-C_6 [26, 32, 33]. To take this fact into consideration in the precrash velocity determination, the probabilistic weights were introduced. The non-centricity has three main sources, one is connected with the geometry of vehicle in question – it may differ from one side to the other. Another aspect is the engine bay equipment, that exhibit asymmetrical stiffness during collision. The final part would be the fact that after the impact the deformed chassis retains its original shape and it does not have to be symmetric between left and right side of the vehicle.

3. Description of B-splines

If $(x_i)_{i=1}^{I}$ is a set of nodes, then:

$$B_i^0(x) = \begin{cases} 1 & if x \in [x_i, x_{i+1}) \\ 0 & otherwise \end{cases} \tag{4}$$

This set is composed of B-splines of order 0 [1, 3]. These are characteristic functions of intervals $[x_i, x_{i+1}]$.

Using recursive formula [31], developed by Carl de Boor, one can design B-splines of order $d \geq 1$:

$$B_i^d(x) = \frac{x - x_i}{x_{i+d} - x_i} B_i^{d-1}(x) + \frac{x_{i+d+1} - x}{x_{i+d+1} - x_{i+1}} B_{i+1}^{d-1}(x) \tag{5}$$

Using B-splines as an approximation gives certain advantages, for instance,

$B_i^d > 0$ is in the range $[x_i, x_{i+d+1}]$ and $B_i^d = 0$ is not in this range. Moreover, following relation takes place:

$$\sum_i B_i^d = 1 \ for\ [x_d, x_{I-d}] \tag{6}$$

Equation 6 can be reiterated as follows: B-splines of the d-order form a partition of one on $[x_d, x_{I-d}]$. What is more, there exists a relationship between the number of nodes, the degree of B-splines and their number:

number of B-splines = number of nodes - degree of B-spline

For example, if we want to consider 2 splines of 3rddegree, we need exactly 5 nodes.

4. Approximation of tensor B-spline products with probabilistic weights

Let a set of points be given $(x_n, y_n, z_n)_{n=1}^{N}$. For the least-square function approximation – functions of two variables, a function family $(h_m)_{m=1}^{M}$ will be used. The goal is to minimize the term (5) by finding the $(a_m)_{m=1}^{M}$ coefficient.

$$\sum_{n=1}^{N} w_n \left(z_n - \sum_{m=1}^{M} a_m h_m(x_n, y_n)\right)^2 \tag{7}$$

Note the entered weights $(w_n)_{n=1}^{N}$, are indirectly mapping the significance of points (x_n, y_n, z_n) i.e. the lower the weight value, the lower the significance of (x_n, y_n, z_n).

If $(a_m)_{m=1}^{M}$, such case is omitted. To choose the weights, following formula should be used:

$$w_n = \frac{number\ of\ points\ (x'_n, y'_n, z'_n)\ with\ |z'_n - z_n| < \frac{Var(z)}{4}}{N} \tag{8}$$

Naturally, clustered points are more significant than the isolated ones (e.g. due to measurement error) and more weight is assigned to those. The following expression proves that a problem of a least-square approximation can be reduced to the solution of a linear equation:

$$\begin{pmatrix} \sum_{n=1}^{N} w_n h_1(x_n, y_n) h_1(x_n, y_n) & \cdots & \sum_{n=1}^{N} w_n h_1(x_n, y_n) h_M(x_n, y_n) \\ \vdots & \ddots & \vdots \\ \sum_{n=1}^{N} w_n h_M(x_n, y_n) h_1(x_n, y_n) & \cdots & \sum_{n=1}^{N} w_n h_M(x_n, y_n) h_M(x_n, y_n) \end{pmatrix} \cdot \begin{pmatrix} a_1 \\ \vdots \\ a_M \end{pmatrix} = \begin{pmatrix} \sum_{n=1}^{N} w_n z_n h_1(x_n) \\ \vdots \\ \sum_{n=1}^{N} w_n z_n h_M(x_n) \end{pmatrix} \tag{9}$$

In this case, tensor products of B-splines takes the role of the function $(h_m)_{m=1}^{M}$. Functions $(f_i)_{i=1}^{5}$ and $(g_j)_{j=1}^{5}$ are the first five B-splines of fourth order.

Following expressions presents 25 tensor products:

$$\begin{gathered} \mathrm{h}_1 = \mathrm{f}_1 \otimes \mathrm{g}_1, \mathrm{h}_2 = \mathrm{f}_1 \otimes \mathrm{g}_2, \mathrm{h}_3 = \mathrm{f}_1 \otimes \mathrm{g}_3,\ \mathrm{h}_4 = \mathrm{f}_1 \otimes \mathrm{g}_4, \\ \mathrm{h}_5 = \mathrm{f}_1 \otimes \mathrm{g}_5, \mathrm{h}_6 = \mathrm{f}_2 \otimes \mathrm{g}_1, \mathrm{h}_7 = \mathrm{f}_2 \otimes \mathrm{g}_2, \mathrm{h}_8 = \mathrm{f}_2 \otimes \mathrm{g}_3, \\ \mathrm{h}_9 = \mathrm{f}_2 \otimes \mathrm{g}_4, \mathrm{h}_{10} = \mathrm{f}_2 \otimes \mathrm{g}_5, \mathrm{h}_{11} = \mathrm{f}_3 \otimes \mathrm{g}_1, \mathrm{h}_{12} = \mathrm{f}_3 \otimes \mathrm{g}_2, \\ \mathrm{h}_{13} = \mathrm{f}_3 \otimes \mathrm{g}_3, \mathrm{h}_{14} = \mathrm{f}_3 \otimes \mathrm{g}_4, \mathrm{h}_{15} = \mathrm{f}_3 \otimes \mathrm{g}_5, \mathrm{h}_{16} = \mathrm{f}_4 \otimes \mathrm{g}_1, \\ \mathrm{h}_{17} = \mathrm{f}_4 \otimes \mathrm{g}_2, \mathrm{h}_{18} = \mathrm{f}_4 \otimes \mathrm{g}_3, \mathrm{h}_{19} = \mathrm{f}_4 \otimes \mathrm{g}_4, \mathrm{h}_{20} = \mathrm{f}_4 \otimes \mathrm{g}_5, \\ \mathrm{h}_{21} = \mathrm{f}_5 \otimes \mathrm{g}_1, \mathrm{h}_{22} = \mathrm{f}_5 \otimes \mathrm{g}_2, \mathrm{h}_{23} = \mathrm{f}_5 \otimes \mathrm{g}_3, \mathrm{h}_{24} = \mathrm{f}_5 \otimes \mathrm{g}_4, \\ \mathrm{h}_{25} = \mathrm{f}_5 \otimes \mathrm{g}_5. \end{gathered}$$

5. Results of approximation of B-spline tensor products

The data set available for mini class is relatively small. This is due to the fact, that mini vehicles are less popular than regular class vehicles. Model is based on 80% of the data set and its validation is performed by using the remaining 20%. Method error has been established by comparing the velocity values of the actual model and its validation, as shown in Figure 2.

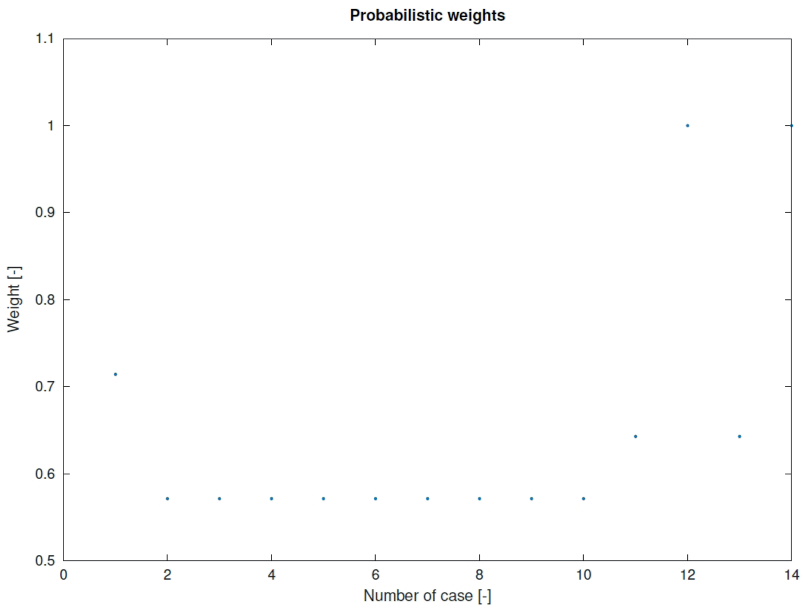

Fig. 2. Probabilistic weight for each individual case

Firstly, probabilistic weights are assigned to each case and introduced into the mathematical model. Then, all the necessary data is inputted, so the model can return values of coefficients $(a_m)_{m=1}^{M}$:

a_1 = -3896.5	a_2 = 5362.1	a_3 = -6883.5
a_4 = 2755.6	a_5 = 3498.4	a_6 = 4678.0
a_7 = -1852.4	a_8 = 2307.7	a_9 = -3123.7

Then a plot of precrash velocity as a function of deformation and mass can be performed, as shown in Figure 3.

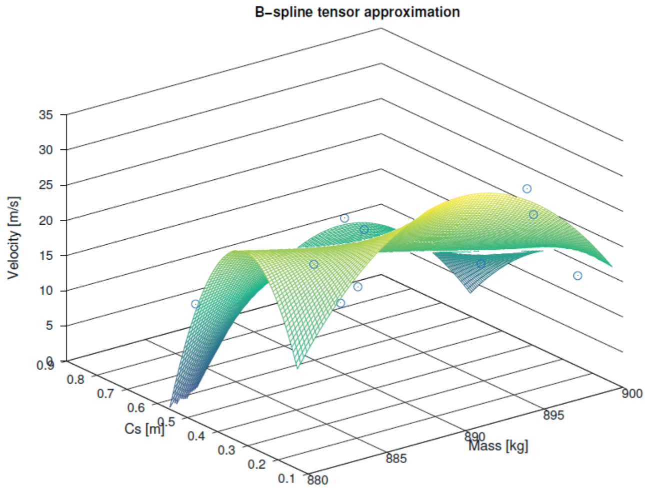

Fig. 3. Approximation of velocity as a function of deformation and mass with B-spline tensor

For comparison, a linear approximation is given by the formula:

$$(\boldsymbol{C_s}, \boldsymbol{m}) \rightarrow \mathbf{7.521549} + \mathbf{12.452939} \cdot \boldsymbol{m} + \mathbf{0.003178} \cdot \boldsymbol{C_s} - (-\mathbf{0.004769}) \cdot \boldsymbol{m} \cdot \boldsymbol{C_s} \ [-] \qquad (10)$$

and is shown in the Figure 4:

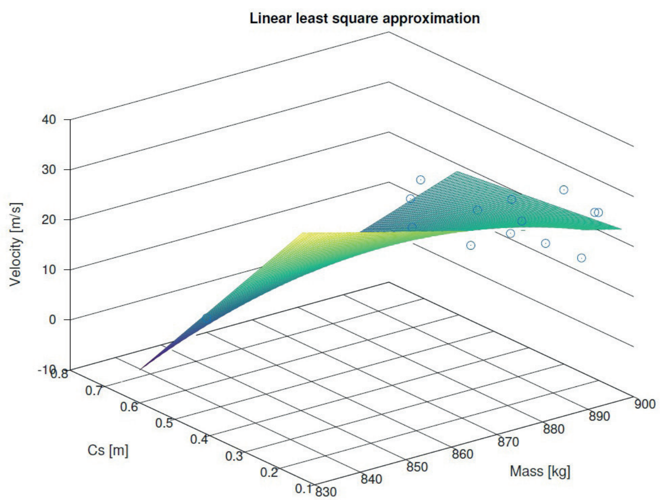

Fig. 4. A linear approximation of the function $V_r = f(m, C_s)$

The B-splines [functions $(f_i)_{i=1}^{3}$] we used in the non-linear model are presented in the Figure 5. The B-splines [functions $(g_j)_{j=1}^{3}$] are presented in the Figure 6.

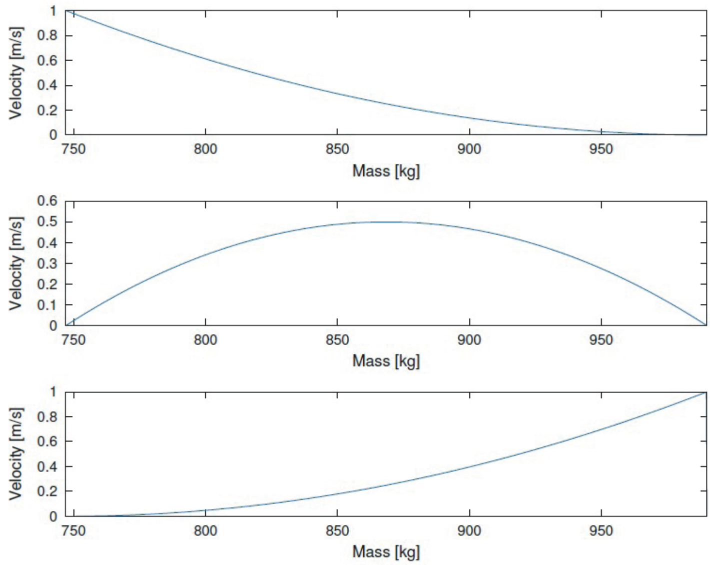

Fig. 5. The B-splines [functions $(f_i)_{i=1}^{3} \equiv V_r = f(m)$ when C_{si} = const] used in the non-linear model

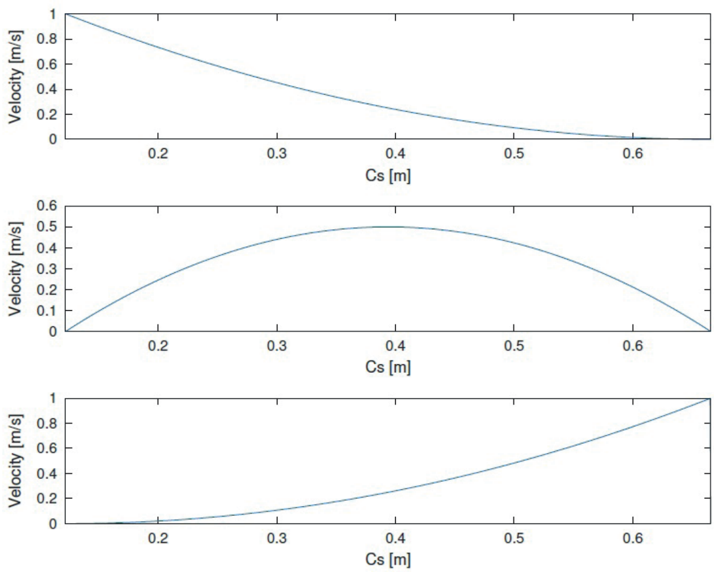

Fig. 6. The B-splines [functions $(g_j)_{j=1}^{3} \equiv V_r = f(C_s)$ when m_j = const] used in the non-linear model

The obtained tensor products of B-splines are shown in the Figure 7.

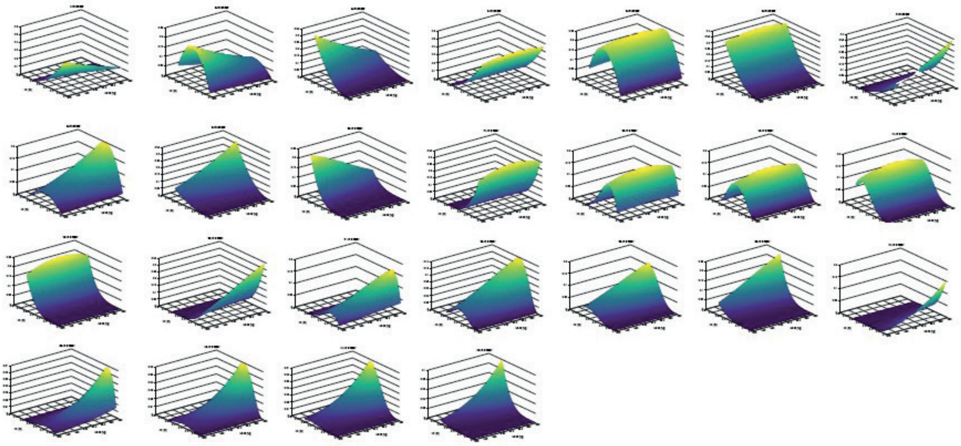

Fig. 7. The obtained tensor products of B-splines used in the non-linear model

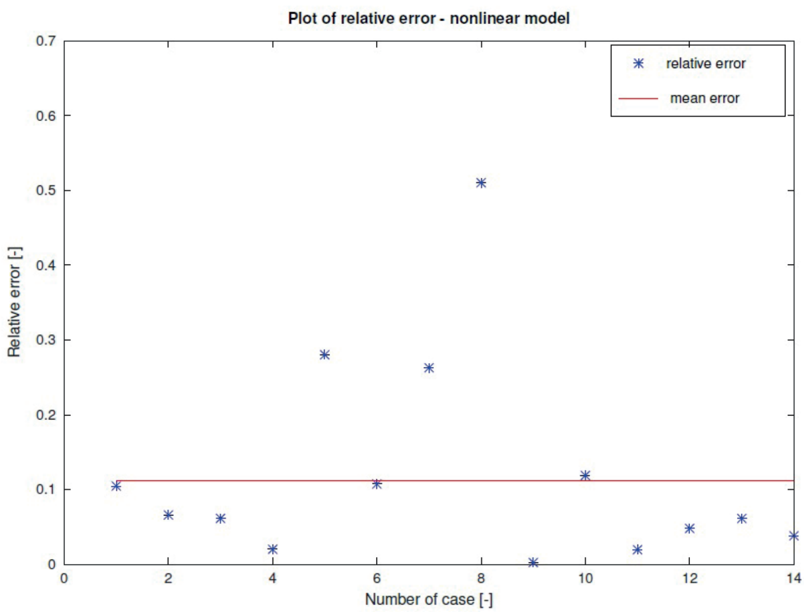

Fig. 8. Plot of relative error – nonlinear model

The obtained values of the error in our method were presented in the Figure 8.

The red line indicates the error of the cases given by the formula:

$$e_{weighted} = \frac{\sum_{n=1}^{N} w_n \left| \frac{B(x_n, y_n) - z_n}{z_n} \right|}{\sum_{n=1}^{N} w_n} \; [-] \tag{11}$$

where B is a B-spline approximating the analyzed points, z_n is the initial value and the whole numerator poses as the relative error in point (x_n, y_n). The relative weighted error for nonlinear approach equates to 11.2%. For comparison, a weighted relative error for the linear model is 18.2%.

Table 2 present chosen cases and compares the linear and nonlinear models. Its contents are summarized in Figure 9.

Tab. 2. Parameters and errors for Mini Car Class

Mass	C_s	V_t	Expected linear	Expected nonlinear	Linear Error	Nonlinear Error
884	0.14	23.25	25.93	25.68	0.11	0.10
896	0.16	25.91	22.97	25.39	0.11	0.02
900	0.25	12.86	21.39	16.24	0.66	0.26
897	0.41	13.13	19.78	14.70	0.50	0.11
880	0.47	16.66	16.33	15.60	0.02	0.06

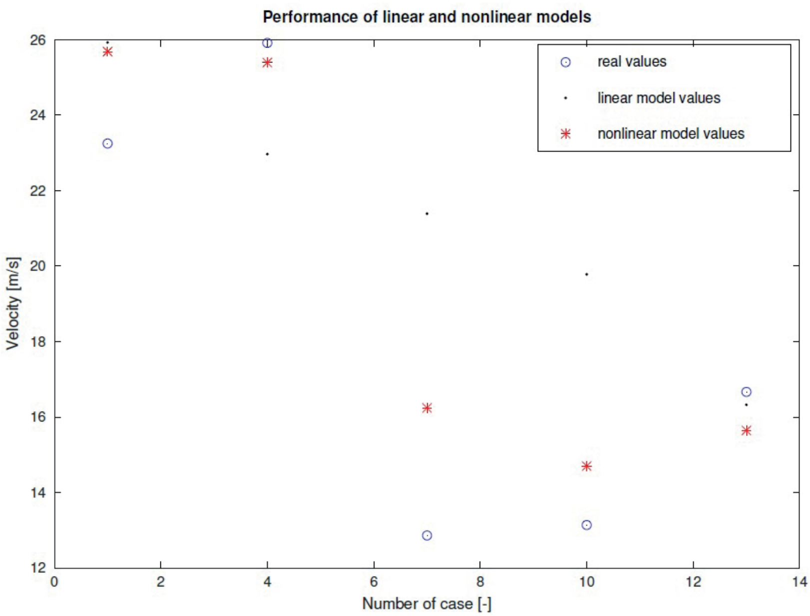

Fig. 9. Performance of linear and non-linear models

6. Conclusions

Author is presenting a new approach to precrash velocity determination. Nonlinear approach proves to be a superior method. Despite a small database, the nonlinear method shows improvement over the linear approach. The mean error for the nonlinear approach is equal to 11.2%, whereas the linear method comes with an error of 18.2%.

Although, the advantage is obvious, this does not mean that this is the finished product. The method can be still further improved, for example by adding more deformation control points, enhancing the deformation profile and thus improving the overall accuracy of the method. Moreover, since this is only a mathematical model, effort is put into developing a standalone app or a device that would present the user with instant value of precrash velocity. This could happen by either manually inputting data needed, like mass, deformation depth, dent zone width, etc. or by 3D scanning the vehicle to limit the manual inputting to a minimum.

7. References

[1] Axler S.: Linear Algebra Done Right. Springer, New York, 1997.

[2] Campbell B.J.: The traffic accident data project scale. InCollision Investigation Methodology Symposium, Warrenton, 1969.

[3] Cheney W., Kincaid D.: Numerical Analysis. Mathematics of Scientific Computing, Wadsworth Group, 2002.

[4] Cromack J.R., Lee S.N.: Consistency study for vehicle deformation index. SAE Technical Paper. 1974, DOI: 10.4271/740299.

[5] Faraj R., Holnicki-Szulc J., Knap L., Seńko J.: Adaptive inertial shock-absorber. Smart Materials and Structures. 2016, 25(3), 035031, DOI: 10.1088/0964-1726/25/3/035031.

[6] Foret-Bruno J.Y., Trosseille X., Le Coz J.Y., Bendjellal F., Steyer C., Phalempin T., et al.: Thoracic injury risk in frontal car crashes with occupant restrained with belt load limiter. SAE Technical Paper. 1998, DOI: 10.4271/983166.

[7] Geigl B.C., Hoschopf H., Steffan H., Moser A.: Reconstruction of occupant kinematics and kinetics for real world accidents. International journal of crashworthiness. 2003, 8(1), 17–27, DOI: 10.1533/ijcr.2003.0217.

[8] Gidlewski M., Żardecki D.: Linearization of the lateral dynamics reference model for the motion control of vehicles. Mechanics Research Communications. 2017, 82, 49–54, DOI: 10.1016/j.mechrescom.2016.09.001.

[9] Gidlewski M., Jemioł L., Żardecki D.: Sensitivity investigations of lane change automated process. 23rd International Conference Engineering Mechanics 2017, Location: Svratka, Czech Republic. Engineering Mechanics. 2017, 23, 330–333, 361–362.

[10] Gidlewski M., Prochowski L.: Analysis of motion of the body of a motor car hit on its side by another passenger car. Scientific Conference on Automotive Vehicles and Combustion 36 Engines (KONMOT), Krakow, Poland. Materials Science and Engineering. 2016, 148, 012039, DOI: 10.1088/1757-899X/148/1/012039.

[11] Gidlewski M., Żardecki D.: Simulation-Based Sensitivity Studies of a Vehicle Motion Model. 20th International Scientific Conference Transport Means 2016, Juodkrante, Lithuania, Transport Means –Proceedings of the International Conference. 2016, 236-240.

[12] Grolleau V., Galpin B., Penin A., Rio G.: Modelling the effect of forming history in impact simulations: evaluation of the effect of thickness change and strain hardening based on experiments. International Journal of Crashworthiness. 2008, 13(4), 363–373, DOI: 10.1080/13588260801976120.

[13] Han I., Kang H., Park J.C., Ha Y.: Three-dimensional crush measurement methodologies using two-dimensional data. Transactions of the Korean Society of Automotive Engineers. 2015, 23(3), 254–262, DOI: 10.7467/KSAE.2015.23.3.254.

[14] Han I.: Analysis of vehicle collision accidents based on qualitative mechanics. Forensic Science International. 2018, 291, 53–61, DOI: 10.1016/j.forsciint.2018.08.004.

[15] Han I.: Vehicle collision analysis from estimated crush volume for accident reconstruction. International Journal of Crashworthiness. 2019, 24(1), 100–105, DOI: 10.1080/13588265.2018.1440499.

[16] Hight P.V., Fugger T.F., Marcosky J.: Automobile damage scales and the effect on injury analysis. SAE Technical Paper. 1992, DOI: 10.4271/920602.

[17] Iraeus J., Lindquist M.: Pulse shape analysis and data reduction of real-life frontal crashes with modern passenger cars. International Journal of Crashworthiness. 2015, 20(6), 535–546, DOI: 10.1080/13588265.2015.1057005.

[18] Krukowski M., Kubiak P., Mrowicki A., Siczek K., Gralewski J.: Non-linear method of determining vehicle pre-crash speed based on tensor B-spline products with probabilistic weights - Intermediate Car Class. Forensic Science International. 2018, 293, 7–16, DOI: 10.1016/j.forsciint.2018.10.011.

[19] Kubiak P.: Work of non-elastic deformation against the deformation ratio of the Subcompact Car Class using the variable correlation method. Forensic Science International. 2018, 287, 47–53, DOI: 10.1016 / j.forsciint.2018.03.033.

[20] Lindquist M., Hall A., Björnstig U.: Real world car crash investigations - A new approach. International Journal of Crashworthiness. 2003, 8(4), 375–384, DOI: 10.1533/ijcr.2003.0245.

[21] Mackay G.M., Hill J., Parkin S., Munns J.A.: Restrained occupants on the nonstruck side in lateral collisions. Accident Analysis & Prevention. 1993, 25(2), 147–152, DOI: 10.1016/0001-4575(93)90054-Z.

[22] Mannering F.L., Bhat C.R.: Analytic methods in accident research: Methodological frontier and future directions. Analytic Methods In Accident Research. 2014, 1, 1–22, DOI: 10.1016/j.amar.2013.09.001.

[23] McHenry B.G.: The algorithms of CRASH. InSoutheast Coast Collision Conference, 2001, 1–34.

[24] McHenry R.: Computer Program for Reconstruction of Highway Accidents. SAE Technical Paper. 1973, 730980, DOI: 10.4271/730980.

[25] Nelson W.D.: The History and Evolution of the Collision Deformation Classification SAE J224 MAR80. SAE Technical Paper. 1981, 810213, DOI: 10.4271/810213.

[26] Neptune J.A.: Crush stiffness coefficients, restitution constants, and a revision of CRASH3 & SMAC. SAE Technical Paper. 1998, 980029, DOI: 10.4271/980029.

[27] Norros I., Kuusela P., Innamaa S., Pilli-Sihvola E., Rajamäki R.: The Palm distribution of traffic conditions and its application to accident risk assessment. Analytic Methods In Accident Research. 2016, 12, 48–65, DOI: 10.1016/j.amar.2016.10.002.

[28] Sharma D., Stern S., Brophy J., Choi E.: An overview of NHTSA's crash reconstruction software WinSMASH. InProceedings of the 20th International Technical Conference on Enhanced Safety of Vehicles. 2007, France.

[29] Siddall D.E., Day T.D.: Updating the vehicle class categories. SAE Technical Paper. 1996, 960897, DOI: 10.4271/960897.

[30] Vangi D., Cialdai C.: Evaluation of energy loss in motorcycle-to-car collisions. International Journal of Crashworthiness. 2014, 19(4), 361–370, DOI: 10.1080/13588265.2014.899072.

[31] Vangi D.: Simplified method for evaluating energy loss in vehicle collisions. Accident Analysis & Prevention. 2009, 41(3), 633–641, DOI: 10.1016/j.aap.2009.02.012.

[32] Wach W., Unarski J.: Determination of vehicle velocities and collision location by means of Monte Carlo simulation method. SAE Technical Paper. 2006, DOI: 10.4271/2006-01-0907.

[33] Wach W., Gidlewski M., Prochowski L.: Modelling reliability of vehicle collision reconstruction based on the law of conservation of momentum and Burg equations. 20th International Scientific Conference Transport Means 2016, Juodkrante, Lithuania. Transport Means – Proceedings of the International Conference. 2016, 693–698.

[34] Wang W., Sun X., Wei X.: Integration of the forming effects into vehicle front rail crash simulation. International Journal of Crashworthiness. 2016, 21(1), 9–21, DOI: 10.1080/13588265.2015.1091170.

[35] Wasik M., Skarka W.: Simulation of Crash Tests for Electrically Propelled Flying Exploratory Autonomous Robot. Advances in Transdisciplinary Engineering. 2016, 4, 937–946, DOI: 10.3233/978-1-61499-703-0-937.

[36] Wood D.P., Simms C.K.: Car size and injury risk: a model for injury risk in frontal collisions. Accident Analysis & Prevention. 2002, 34(1), 93–99, DOI: 10.1016/S0001-4575(01)00003-3.

[37] Żuchowski A.: The use of energy methods at the calculation of vehicle impact velocity. Archiwum Motoryzacji. 2015, 68, 85–111, 197–222.